Article

Methane to Liquid Hydrocarbons over Tungsten-ZSM-5 and Tungsten Loaded Cu/ZSM-5 Catalysts

Didi Dwi Anggoro[1]*,   Nor Aishah Saidina Amin[2]

1. Department of Chemical Engineering, University of Diponegoro Tembalang, Semarang 50239, Indonesia;
2. Faculty of Chemical and Natural Resources Engineering, Universiti Teknologi Malaysia,
Johor Bahru 81130, Malaysia

Abstract: Metal containing ZSM-5 can produce higher hydrocarbons in methane oxidation. Many researchers have studied the applicability of HZSM-5 and modify ZSM-5 for methane conversion to liquid hydrocarbons, but their research results still lead to low conversion, low selectivity and low heat resistance. The modified HZSM-5, by loading with tungsten (W), could enhance its heat resistant performance, and the high reaction temperature (800 °C) did not lead to a loss of the W component by sublimation. The loading of HZSM-5 with tungsten and copper (Cu) resulted in an increment in the methane conversion as well as CO_2 and C_{5+} selectivities. In contrast, CO, C_{2-3} and H_2O selectivities were reduced. The process of converting methane to liquid hydrocarbons (C_{5+}) was dependent on the metal surface area and the acidity of the zeolite. High methane conversion and C_{5+} selectivity, and low H_2O selectivity are obtained over W/3.0Cu/HZSM.

Key words: methane; liquid hydrocarbons; HZSM-5; W-ZSM-5; W-Cu/ZSM-5

1. Introduction

In general, there are two routes for converting methane to gasoline: indirectly or/and directly. The indirect route is a two-step process whereby natural gas is first converted into synthesis gas (a mixture of H_2 and CO), and then into hydrocarbons of the gasoline range. The direct route is a one step process in which the natural gas reacts with oxygen (or another oxidizing species) to give the desired product directly.

The use of the HZSM-5 zeolite as a support of the metal oxide phase is very interesting due to three reasons: its thermal stability, its high surface area that enables high metal oxide loading and the presence of acid sites that could lead to the formation of certain active metal oxide species [1].

Ernst and Weitkamp [2] reported in a paper on the conversion of methane over zeolite-based catalysts that the presence of strong acid sites in the zeolite catalyst is detrimental for the selective oxidation of methane to higher hydrocarbons; otherwise oxidized products of CO_x (CO, CO_2) will predominate. When the acidity is reduced by exchanging the zeolite with alkali metal cations, the selectivity to higher hydrocarbons is slightly enhanced. Han et al. [3] demonstrated the successful production of higher hydrocarbons from methane oxidation using a ZSM-5 zeolite catalyst containing metal oxides. The metal oxides with sufficiently high dehydrogention and low olefin oxidation activities reduce the acidity of the ZSM-5. As a result, the metal containing ZSM-5 can produce higher hydrocarbons in methane oxidation.

De Lucas et al. [1,4,5] discovered that the introduction of Cu(II) ions by an ion-exchange method

could remarkably increase the activity of Mo/HZSM-5 for methane aromatization and improve its stability to some extent. Mo species is the most active component for methane non-oxidative aromatization so far, but its activity and stability need to be improved. Xiong *et al.* [6,7] studied the incorporation of metals Zn, Mn, La, and Zr into the W/HZSM-5 catalyst. Under reaction condition of 0.1 MPa, 1073 K, GHSV of feed gas CH_4 and 10% Argon at 960 h^{-1}, the conversion of methane reached 18% 23% in the first two hours of reaction, and the corresponding selectivity to benzene, naphthalene, ethylene and coke was 48% 56%, 18%, 5% and 22%, respectively. Ding *et al.* [8] reported the non-oxidative methane reaction over W/HZSM-5 to produce C_2 C_{12} hydrocarbons. Under the condition of 700 °C, flow rate CH_4 and Argon at 12.5 cm^3/min, the C_2 C_{12} selectivity was 70%–80%. However, the methane conversion was low, just between 2% and 3%. On the basis of the chemical similarities between MoO_3 and WO_3, it seems reasonable to expect a parallelism in their catalytic properties. Mo species is the most active component for methane non-oxidative aromatization so far, but its activity and stability need to be improved. Recently, we have found that the introduction of Cu(II) ions by an ion-exchange method can remarkably increase the activity of Mo/HZSM-5 for methane aromatization and can improve its stability to some extent.

Cu loaded ZSM-5 catalysts *via* acidic ion exchange method have been identified to be potential catalysts for the conversion of methane to liquid fuels [9]. However, infrared study of metal loaded ZSM-5 catalysts indicated that the catalysts are not resistant to high temperatures. Previous studies have indicated that metal loaded ZSM-5 did not exhibit the vibration band at 3610 cm^{-1} and 3660 cm^{-1}, except for the ZSM-5 which showed a weak vibration band at 3666 cm^{-1}. The result suggested that framework and non-framework aluminum were either extracted to the acidic solution or changed to silanol defect form when calcined at 800 °C and made the catalysts inactive [10]. In our previous studies [11,12] it was indicated that the Cu loaded W/ZSM-5 catalyst was thermally stable at the reaction temperature (700–800 °C).

In this study ZSM-5 was modified with tungsten and copper and the catalyst performance was tested for the oxidation of methane to liquid hydrocarbons. The catalysts were characterized by XRD, TPR, TPD and N_2 Adsorption measurements. We would like to investigate the resistivity of tungsten modified HZSM-5 to high temperatures and its cat-alytic activity for the conversion of methane.

2. Experimental

2.1. Preparation of catalysts

ZSM-5 zeolite with a SiO_2/Al_2O_3 mole ratio of 30 was supplied by Zeolyst International Co, Ltd, Netherlands. The surface area of the zeolite is 400 m^2/g. The W (3% weight)-HZSM-5 catalyst was prepared by impregnating a certain amount of the HZSM-5 zeolite carrier with an ammonium tungstate hydrate solution [6,7]. The ammonium tungstate hydrate solution was prepared by dissolving $(NH_4)_2WO_4$ in deionized water and adding a small amount of H_2SO_4 to regulate the pH value of the solution to 2 3. The sample (10 ml of solution *per* gram zeolite) was dried in an oven at 120 °C for 2 h and then calcined at 500 °C for 4 h.

The W loaded Cu/HZSM-5 was prepared by first impregnating a certain amount of the HZSM-5 zeolite carrier with a calculated amount of copper nitrate in aqueous solutions, followed by drying at 120 °C for 2 h and calcining at 400 °C for 4 h, and subsequently impregnating with a calculated amount of H_2SO_4 acidified $(NH_4)_2WO_4$ aqueous solution (pH=2 3). Finally, the sample was dried at 120 °C for 2 h and calcined at 500 °C in air for 5 h.

2.2. Characterization and testing of catalysts

X-ray diffraction (XRD), H_2-temperature programmed reduction (H_2-TPR), NH_3-temperature programmed desorption (NH_3-TPD), N_2 adsorption and FT-IR were utilized for the characterization of the catalysts. XRD and FT-IR were employed to determine the zeolite structure. NH_3-TPD provided the acidity of the catalyst samples. H_2-TPR data were pertinent to the zeolite morphology.

The performance of the catalysts was tested for methane conversion to liquid hydrocarbons (LHC) *via* a single step reaction in a fixed-bed micro reactor. Methane with 99.9% purity was reacted at atmospheric pressure and various temperatures and oxygen concentration. An on-line gas chromatography with a TCD and a Porapak-N column was utilized to analyze the gas. The liquid product was analyzed using the GC FID and an HP-1 column.

3. Results and discussion

3.1. Characterization of catalysts

X-ray diffraction (XRD) and nitrogen adsorption (NA) were employed to determine the morphology of the catalysts. The XRD diffractograms of HZSM-5, W/HZSM-5 and W loaded Cu/HZSM-5 catalysts with different Cu loadings calcined at 550 °C are shown in Figure 1. The peaks at $2\theta=41°$ indicated tungsten oxides [13] whilst copper oxides are indicated at $2\theta=34°$. The intensities of these peaks increased with increasing copper loading.
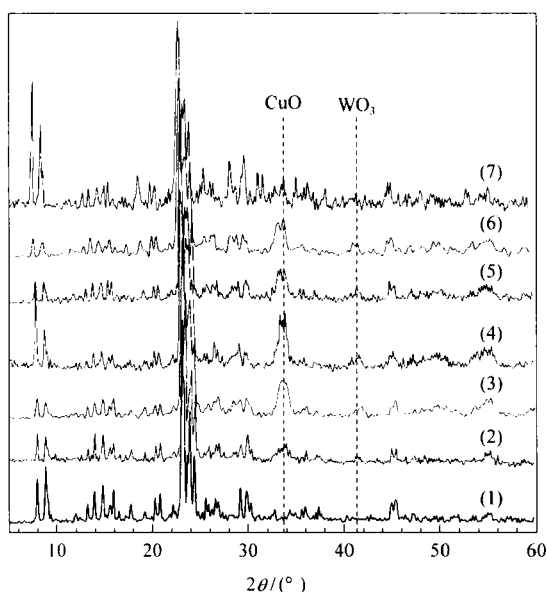

Figure 1. XRD pattern of different HZSM-5 catalysts
(1) HZSM-5, (2) W/HZSM-5, (3) W/0.5Cu/HZSM-5,
(4) W/1.0Cu/HZSM-5, (5) W/1.5Cu/HZSM-5,
(6) W/2.0Cu/HZSM-5, (7) W/3.0Cu/HZSM-5

The crystallinity values calculated from the XRD diffractograms and the areas of the samples from NA analysis are tabulated in Table 1. The crystallinities of W/1.0Cu/HZSM-5, W/2.0Cu/HZSM-5 and W/3.0Cu/HZSM-5 are 89%, 88% and 69%, re-

spectively. These values are lower compared to the values of other samples. All the metal and bi-metal ZSM-5 zeolite catalysts have surface and micropore areas smaller than the parent zeolite. The reduction in surface area of the metal-loaded HZSM-5 indicates a strong interaction between the surface of the zeolite and the copper and tungsten species, which enables a good dispersion of the metals on the surface [5]. Among the samples, the BET surface area and the micropore area of W/3.0Cu/HZSM-5 are the lowest, being 236 m^2/g and 213 m^2/g, respectively.

Table 1. Crystallinity and surface area of the catalysts

Catalyst	Crystallinity (%)	BET surface area (m^2/g)	Micropore area (m^2/g)
HZSM-5	100	403	373
W/HZ	100	280	257
W/0.5Cu/HZ	94	266	243
W/1.0Cu/HZ	89	286	261
W/1.5Cu/HZ	101	267	244
W/2.0Cu/HZ	88	285	260
W/3.0Cu/HZ	69	236	213

The results in Table 2 pertain to the total volume, micropore volume, average pore diameter and acidity of the catalysts. Tungsten and copper species easily entered or partially blocked the channels of the ZSM-5 zeolite pores and thus, reduced the volume of the catalysts. The average pore diameters of the metal-loaded HZSM-5 zeolites are larger than the parent zeolite, as revealed by the results in Table 2. The average pore diameter of the W/3.0Cu/HZSM-5 is the largest, and as indicated in Table 2, the percentage of micropore volume in the catalyst surface has been reduced to 50%.

Table 2. Total volume, pore distribution and acidity of the catalysts

Catalyst	Total volume (cm^3/g)	Micropore volume (cm^3/g)	Ratio of micropore to total volume (%)	Average pore diameter (Å)	Acidity (mol/kg)
HZSM-5	0.245	0.149	61	24.3	0.87
W/HZ	0.187	0.106	57	26.8	0.81
W/0.5Cu/HZ	0.176	0.101	57	26.5	0.91
W/1.0Cu/HZ	0.175	0.110	63	24.4	1.01
W/1.5Cu/HZ	0.179	0.101	56	26.9	1.01
W/2.0Cu/HZ	0.191	0.109	57	26.6	0.98
W/3.0Cu/HZ	0.176	0.088	50	29.8	1.19

The ammonia-TPD spectra of the catalyst provided useful information about the intensity and the concentration of the acid sites on the catalyst surface, as tabulated in Table 2. The concentration of the surface acid sites (acidity) of the metal-loaded HZSM-5 is higher than that of the ZSM-5 zeolite.

This could probably be attributed to the average pore diameters of the metal-loaded HZSM-5 which are larger than the pore diameters of the HZSM-5 zeolite itself, as shown in Figure 2. This is similar with the results of Koval *et al.* (1996). They reported that the acidity decreased with the decreasing micropore volume of HZSM-5 [14]. As revealed by the result in Figure 2, the strongest acidity shown by the W/3.0Cu/HZSM-5 zeolite coincides with the fact that it has the largest pore diameter (29.8 Å). However, the acidity of the W/1.0Cu/HZSM-5 is higher (1.01 mol/kg) than HZSM-5 (0.87 mol/kg), although the difference in pore size between W/1.0Cu/HZSM-5 and HZSM-5 is not large.
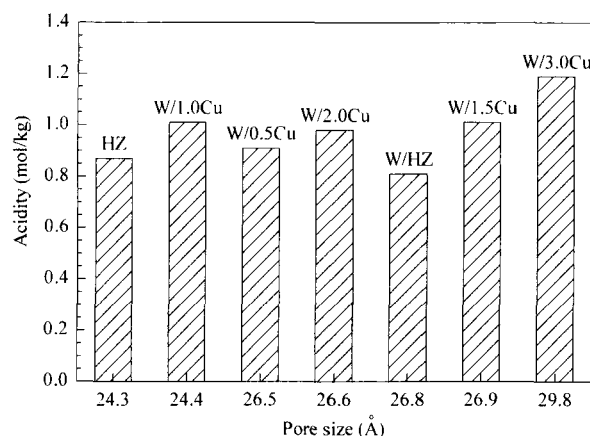

Figure 2. Effect of pore size on acidity of catalysts

Figure 3 depicts the ammonia-TPD spectra of the HZSM-5, W/HZSM-5 and W loaded Cu/HZSM-5 with different amounts of Cu loading. For the HZSM-5 and W/HZSM-5, the ammonia-TPD peaks appeared at about 250 °C and about 430 °C, which may be ascribed to the desorption of two kinds of ammonia species adsorbed on weak acid (mostly Lewis acid) sites and strong acid (mostly Brönsted acid) sites, respectively [15].

The addition of 0.5% Cu to HZSM-5 led to a reduction of the intensity of the high temperature (~ 430 °C) peak and a small downshift of its position, as revealed in Figure 3. When the amount of Cu loading was increased to 1.0%, the high temperature peak disappeared, indicating that most of the surface Brönsted acid sites had vanished. However, as the copper loading was further increased to 1.5% and 3.0%, the ammonia-TPD peaks appeared again at ~ 430 °C. One interesting feature of Figure 3 is the ammonia-TPD spectra of the W/2.0Cu/HZSM-5 that indicated a peak at 400 °C (Figure 3 (6)). This small peak may be attributed to the emergence of

medium strength Brönsted acid sites. This is similar with the results found by previous researchers [6-7], where the incorporation of Mg^{2+} and Zn^{2+} into the W/HZSM-5 host catalyst resulted in the elimination of strong surface Brönsted acid sites and the generation of new medium-strength acid sites.
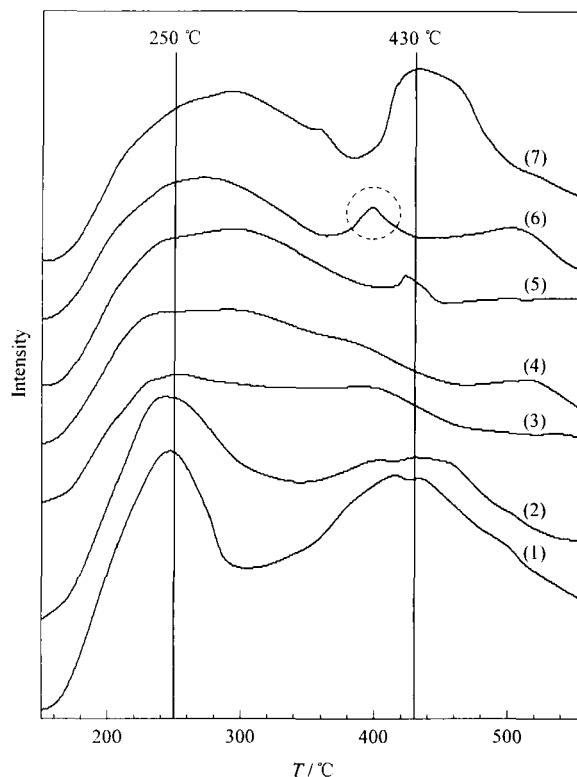

Figure 3. Ammonia-TPD spectra of different HZSM-5 catalysts
(1) HZSM-5, (2) W/HZSM-5, (3) W/0.5Cu/HZSM-5,
(4) W/1.0Cu/HZSM-5, (5) W/1.5Cu/HZSM-5,
(6) W/2.0Cu/HZSM-5, (7) W/3.0Cu/HZSM-5

The migration of the W and Cu species was indirectly studied by infrared (IR) spectroscopy. W/HZSM-5 and W/Cu/HZSM-5 samples showed in the OH stretching vibration three IR bands at ≈ 3610 cm^{-1}, due to bridge Si-OH (Al) acidic groups, at ≈ 3660 cm^{-1} due to non-framework Al sites, or octahedral, and at ≈ 3740 cm^{-1} which is attributed to terminal Si-OH non-acidic groups [10]. The vibrations for the (OH) region of the IR spectra of the W/HZSM-5 and W/3.0Cu/HZSM-5 zeolite catalysts are shown in Figure 4, where all the fresh samples have bands at ≈ 3610 cm^{-1}, ≈ 3660 cm^{-1}, and ≈ 3740cm^{-1}. The spectra indicated that all the samples have aluminum framework, silanol, and aluminum non-framework groups. In addition, the IR spectra demonstrated that the intensity of the band at about 3610 cm^{-1} of fresh W/HZSM-5 is stronger

than fresh W/3.0Cu/HZSM-5. This is probably due to the W or W and Cu species that have migrated in the zeolite framework and occupied the H^+ position. It resulted in a large decrement of the 3610 cm^{-1} IR band intensity, as shown in Figure 4 (3).
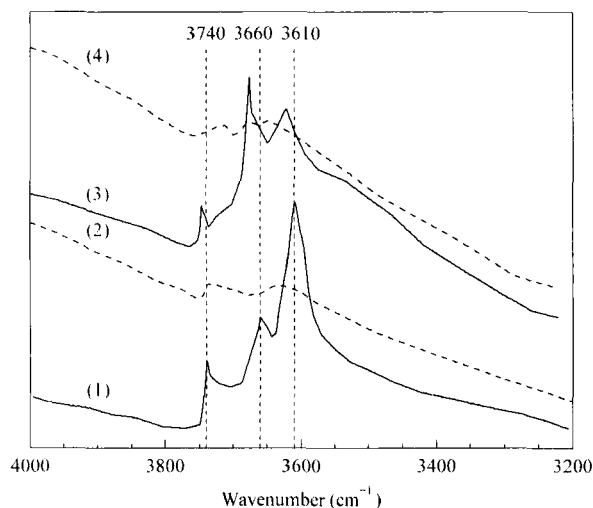

Figure 4. IR spectra in the OH region of fresh and used catalysts
Fresh (1) W/HZSM-5 and (3) W/3.0Cu/HZSM-5, used (2) W/HZSM-5 and (4) W/3.0Cu/HZSM-5 for reaction at 800 °C

It is clear that the roles of W on W/HZSM-5 and W and Cu on W/Cu/HZSM-5 is to reduce the amount of Brönsted acid sites. The amount of Brönsted acid sites (N_{BAC}) can be calculated by bridging the OH groups (at 3609 cm^{-1} band) according to [10,16]. The N_{BAC} for the HZSM-5, W/HZSM-5 and W/3.0Cu/HZSM-5 are 2.9 μmol/g, 0.5 μmol/g and 0.3 μmol/g, respectively.

Further reaction with methane and oxygen at 800 °C for five hours resulted in the disappearance of the band at about 3610 cm^{-1} for both of the W/HZSM-5 and W/Cu/HZSM-5 samples (Figures 4 (2) and 4 (4)). This is probably due to the extraction of aluminum in the zeolitic framework into the non-framework or due to the deposition of carbonaceous residues. The deposition of coke led to catalyst deactivation after five hours of reaction.

The TPR profiles of W/HZSM-5 and W loaded Cu/HZSM-5 catalysts are depicted in Figure 5. As observed, all the curves contain several peaks in the temperature range of 200–900 °C. The TPR patterns of all catalysts exhibited two peaks, with the maximum at 700 °C and 780 °C. These peaks may be ascribed to the two subsequent steps of single-electron reduction of the W^{6+} species derived from the $(WO_4)^{2-}$ precursor with tetrahedral coordina-

tion, $W^{6+}+e^-{\rightarrow}W^{5+}$ and $W^{5+}+e^-{\rightarrow}W^{4+}$ [17]. The reducibility of this type of catalyst decreased as the strength of the interaction between the metal oxide species and the surface of the support increased. The existence of a single reduction peak at 550 °C for W/HZSM-5, W/0.5Cu/HZSM-5 and W/1.0Cu/HZSM-5 samples may be due to the single electron reduction of the W^{6+} species derived from the $(WO_6)^{n-}$ precursor with octahedral coordination, $W^{6+}+e^-{\rightarrow}W^{5+}$ [6,7]. This peak (at 550 °C) disappeared if the amount of Cu loading on the HZSM-5 was more than 1.0 wt%. The observed hydrogen-TPR peak at 370 °C could be due to the reduction of Cu^{n+} species and the intensity of the peak became stronger as the copper loading increased.
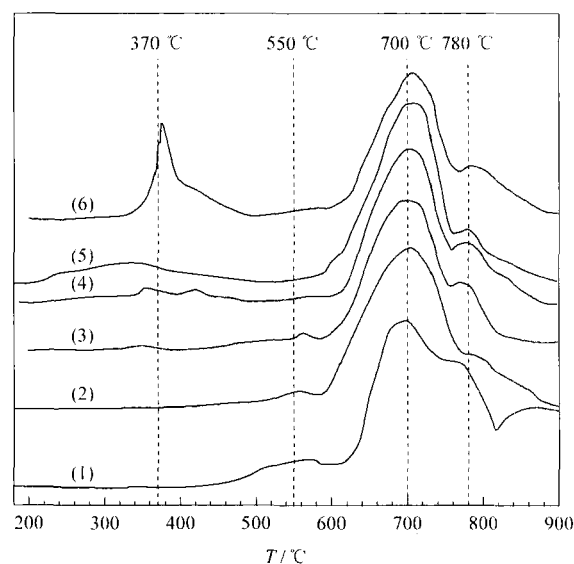

**Figure 5. Hydrogen-TPR spectra of different HZSM-5 catalysts**
(1) W/HZSM-5, (2) W/0.5Cu/HZSM-5, (3) W/1.0Cu/HZSM-5, (4) W/1.5Cu/HZSM-5, (5) W/2.0Cu/HZSM-5, (6) W/3.0Cu/HZSM-5

In Table 3 the quantitative results of the TPR is summarized. The TPR software automatically calculated the metal surface area, dispersion of metal, and mean particle diameter basing on W and Cu for the bimetallic W/Cu/HZSM-5 catalysts in the experimental part. The tungsten content for all catalysts is constant. The copper content and percent of copper dispersed for W/Cu/HZSM-5 catalysts increased with increasing copper concentration. Such small particles (0.03–0.05 nm or 3–5 Å), particularly the tungsten particles, should be localized to inside the zeolite pores [18], where the pore diameter of ZSM-5 is about 5.6 Å.

Table 3. Metal state in the reduced catalysts

Catalyst	Metal content (μmol/g)		Metal surface area (m^2/g)		Dispersion of metal (%)		Mean particle diameter (nm)	
	W	Cu	W	Cu	W	Cu	W	Cu
W/HZ	163	—	2.66	—	55	—	0.0518	—
W/0.5Cu/HZ	163	79	6.02	0.04	100	24	0.0287	1.559
W/1.0Cu/HZ	163	157	4.00	0.07	68	22	0.0419	1.721
W/1.5Cu/HZ	163	236	3.11	0.16	65	40	0.0444	0.930
W/2.0Cu/HZ	163	315	4.18	0.48	76	79	0.0379	0.475
W/3.0Cu/HZ	163	472	4.77	0.92	86	100	0.0332	0.373

The percentage of metal dispersion in Table 3 reveals that Cu is 100% dispersed for the W/3.0Cu/HZSM-5 sample. Figure 6 shows that the BET surface area of all the samples decreased with increasing dispersion of Cu except for the W/2.0Cu/HZSM-5. This is probably due to some tungsten or copper species on W/2.0Cu/HZSM-5 that have formed tungsten oxide or copper oxide on the zeolite surface.
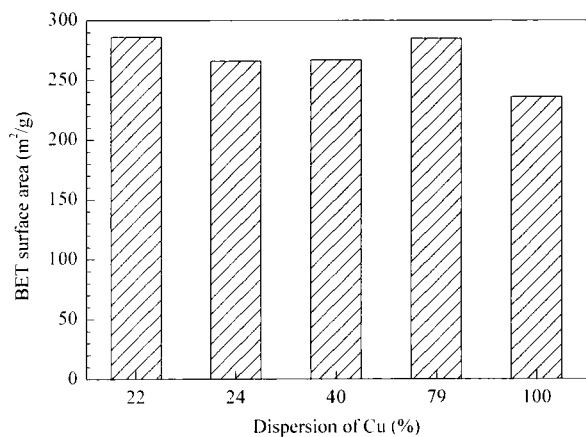
Figure 6. Effect of dispersion of Cu (%) on BET surface area of catalysts

The results in Table 3 indicated the dispersion of Cu on the W/1.0Cu/HZSM-5 is the smallest (about 22%) compared to the other samples, owing to the largest mean particle diameter of Cu (1.721 nm) on W/1.0Cu/HZSM-5. The small percentage of Cu being dispersed on the W/1.0/HZSM-5 catalyst led to only a small amount of Cu ions being exchanged with H$^+$. As a consequence, the acidity of the W/1.0/HZSM-5 is high (1.01 mol/kg), although its pore size is small (24.4 Å). It is clear that the role of Cu on the W/Cu/HZSM-5 is not only to reduce the W^{6+} species derived from the $(WO_6)^{n-}$ precursor with octahedral coordination, but also to have an effect on the acidity of the ZSM-5 zeolite, as revealed by the ammonia-TPD result.

The TPR profiles of W loaded 3.0Cu/HZSM-5 catalysts before and after reaction are depicted in Figure 7. The spectra demonstrated the existence of a single reduction peak of Cu oxide at 370 °C. However, after reaction at 800 °C the peak disappeared, probably due to the reduction of Cu^{n+}. This is probably due to the partial oxidation of the catalyst during the reaction.
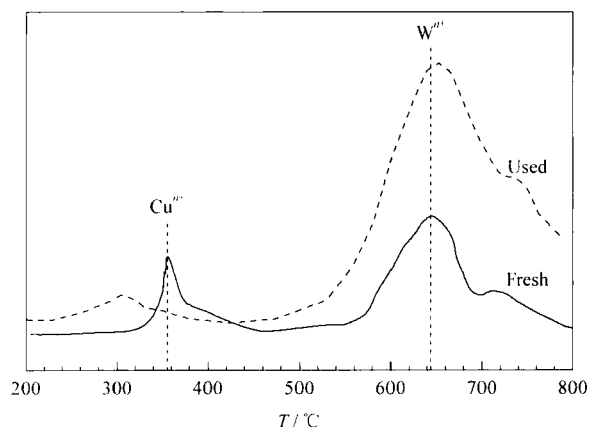
Figure 7. Hydrogen-TPR spectra of W/3.0Cu/HZSM-5 catalyst before and after reaction at 800 °C

Nevertheless, the peak of W^{n+} did not change before and after the reaction. The TPR profile for tungsten revealed that the addition of tungsten has increased the thermal stability of the catalyst, as the W component has not lost due to sublimation after reaction at 800 °C.

3.2. Performances of catalysts

The methane conversion increased due to the increasing copper content and copper surface area. This result demonstrated that the methane conversion is related to the copper surface area, as shown in Figure 8. The methane conversion of HZSM-5 is about 13% and increased to 21% at copper surface area of

0.92 m^2/g for W/3.0Cu/HZSM-5 (Table 3). However, methane conversion over the W/1.0Cu/HZSM-5 is lower than over the W/0.5Cu/HZSM-5, although the Cu surface area of the former is larger. It is clear that the dispersion of Cu on the active surface of the catalyst affected the methane conversion. Since the percentage of Cu dispersed on the catalyst surface is the smallest for W/1.0Cu/HZSM-5 (see Table 3) the methane conversion is the lowest using this catalyst.
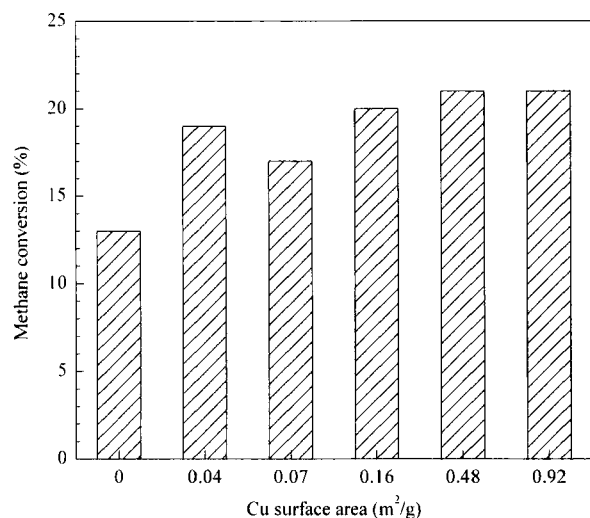

Figure 8. Effect of Cu BET surface area on methane conversion

The products of the reaction between methane and oxygen over HZSM-5, W/HZSM-5 and W/Cu/HZSM-5 with different concentrations of copper are C_2H_2, C_2H_4, C_2H_6, C_3H_6, CO, CO_2, H_2O and liquid hydrocarbons. Figure 9 summarizes the product selectivities of all the catalysts. The results in Figure 9 shows that over HZSM-5 and metal loaded HZSM-5, the selectivity to carbon monoxide is higher than that of carbon dioxide. This indicates that the partial oxidation of methane has occurred with carbon monoxide and hydrogen as the products. However, hydrogen possibly reacted with carbon dioxide to form water in the Reversed Water Gas Shift (RWGS) reaction.

The water selectivity of HZSM-5 is higher than the metal loaded HZSM-5, because the HZSM-5 catalyst has no metal content or metal surface area, while the metal loaded HZSM-5 catalysts have tungsten oxide and copper oxide contents. Over tungsten oxide or copper oxide the reaction of hydrogen and carbon monoxide produced hydrocarbon gases (C_2 and C_3), which could oligomerize to liquid hydrocarbons (C_{5+}) in the presence of the HZSM-5 zeolite catalyst.

The selectivity for C_2–C_3 hydrocarbons for all

catalysts is very low (1%–2%), as depicted in Figure 9. This is probably due to that all catalysts enhanced the oligomerization of C_2 hydrocarbons to C_{5+} liquid hydrocarbons and reduced the amount of C_2-C_3 hydrocarbons. The C_{5+} hydrocarbons selectivity increased with increasing acidity, as shown in Figure 10. The selectivity to C_{5+} hydrocarbons using W/3.0Cu/HZSM-5 is the highest (34%), owing to its highest acidity (1.19 mol/kg) and copper surface area (0.92 m^2/g) among other samples.
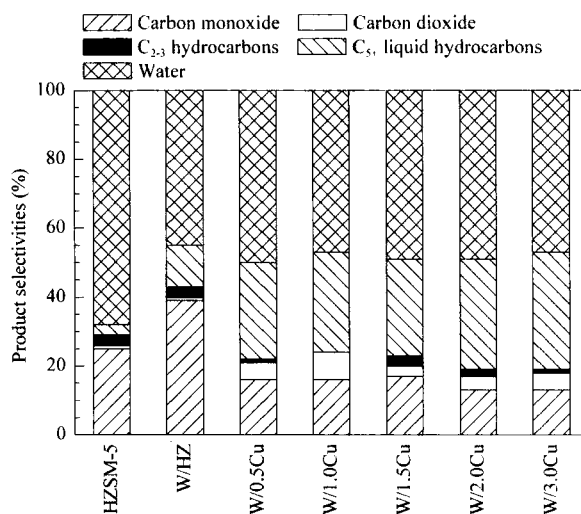

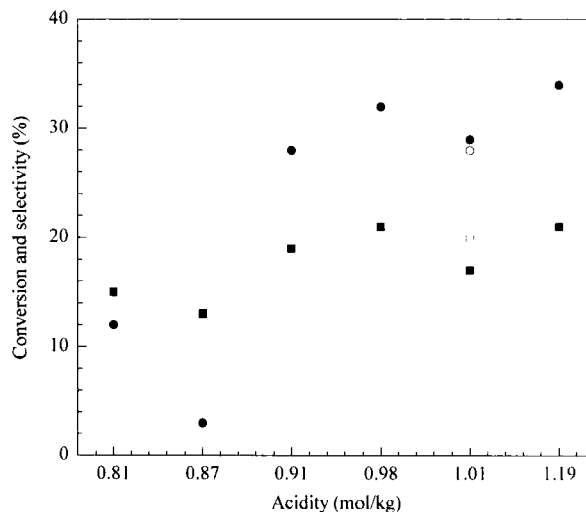Figure 9. Distribution of product selectivities over different catalysts

Figure 10. Effect of acidity on methane conversion and liquid hydrocarbons C_{5+} selectivity

(■) methane conversion, (●) C_{5+} selectivity,
(□) methane conversion over W/1.5Cu/HZSM-5,
(○) C_{5+} selectivity over W/1.5Cu/HZSM-5

The result in Table 4 indicates that the composition of C_{5-10} hydrocarbons increased as the num-

ber of Brönsted acid sites (N_{BAC}) decreased. The gasoline range (C_{5-10}) composition of ZSM-5 was about 96% at a N_{BAC} value of 2.9 and increased to 100% with N_{BAC} equal to 0.3 for the W/3.0Cu/ZSM-5 sample (Table 4). From the ammonia-TPD (Figure 4) spectra the strength of Brönsted acid sites of W/3.0Cu/ZSM-5 is the strongest among others. These results suggest that higher composition of gasoline formed from methane depends on the strength of Brönsted acid sites.

Table 4. Number of Brönsted acid sites and composition of C_{5-10} and C_{11+} hydrocarbons over HZSM-5, W/ZSM-5 and W/3.0Cu/ZSM-5

Catalyst	No. of Brönsted acid sites (N_{BAC}) (μmol/g)	Composition (%) C_5-C_{10}	C_{11+}
HZSM-5	2.9	96	4
W/HZSM-5	0.5	99	1
W/3.0Cu/HZSM-5	0.3	100	0

4. Conclusions

The loading of HZSM-5 with tungsten and copper decreased the crystallinity, surface area, and also total volume of the catalysts. However, the average pore diameter and the acidity of the zeolites increased as a result of the modification with the metals. Such metal particles are smaller than the average pore size, and the metal particles should be localized to the inner side of the zeolite pores. TPR patterns indicated that modified HZSM-5 by loading with tungsten enhanced its heat resistant performance, so the high reaction temperature (800 °C) did not lead to loss of the W component by sublimation.

While loading HZSM-5 with tungsten and copper enhanced the methane conversion, CO_2 and C_{5+} products, however, reduced the CO, C_{2-3}, and H_2O selectivities. The process of converting methane to liquid hydrocarbons (C_{5+}) is dependent on the metal surface area and the acidity of the zeolite. The W/3.0Cu/HZSM-5 is the potential catalyst, because over this catalyst high methane conversion and C_{5+} selectivity, and low H_2O selectivity are obtained.

References

[1] de Lucas A, Valverde J L, Canizares P, Rodriguez L. *Appl Catal A: General*, 1998, **172**: 165

[2] Ernst S, Weitkamp J. Hydrocarbons Source of Energy. Imarisio G, Frias M, Bemtgen J M(Editors). London: Graham & Trotman, 1989. 461

[3] Han S, Martenak D J, Palermo R E, Pearson J A, Walsh D E. *J Catal*, 1994, **148**: 134

[4] de Lucas A, Valverde J L, Canizares P, Rodriguez L. *Appl Catal A*, 1999, **184**: 143

[5] de Lucas A, Valverde J L, Rodriguez L, Sanchez P, Garcia M T. *J Mol Catal A*, 2001, **171**: 195

[6] Xiong Z T, Cheng L L, Zhang H B, Zeng J L, Lin G D. *Catal Lett*, 2001, **74**: 227

[7] Xiong Z T, Zhang H B, Lin G D, Zeng J L. *Catal Lett*, 2001, **74**: 233

[8] Ding W, Meitzner G D, Marler D O, Iglesia E. *J Phy Chem B*, 2001, **105**: 3928

[9] Amin N A S, Anggoro D D. *J Natur Gas Chem*, 2003, **12**(2): 123

[10] Amin N A S, Anggoro D D. *J Natur Gas Chem*, 2002, **11**: 79

[11] Amin N A S, Anggoro D D. Proceedings of the Conference on Chemical and Bioprocess Engineering. Sabah, Malaysia, 2003

[12] Amin N A S, Anggoro D D. *Fuel*, 2004, **83**: 487

[13] Logie V, Wehrer P, Katrib A, Maire G. *J Catal*, 2000, **189**: 438

[14] Koval L M, Gaivoronskaya Yu I, Patrushev Yu V. *Russian J Appl Chem*, 1996, **69**(2): 235

[15] Woolery G L, Kuehl G H, Timken H C, Chester A W, Vartuli J C. *Zeolites*, 1997, **19**: 288

[16] Wichterlova B, Tvaruzkova Z, Sobalik Z, Sarv P. *Microporous Mesoporous Mater*, 1998, **24**: 223

[17] Shu Y, Xu Y, Wong S T, Wang L, Guo X. *J Catal*, 1997, **170**: 11

[18] Hoang D L, Berndt H, Miessner H, Schreier E, Völter J, Lieske H. *Appl Catal A: General*, 1994, **114**: 295